


Dissecting the role of toll-like receptor 7 in pancreatic cancer

Maren Stark¹ | Marina Nicolai² | Marina Tatura¹  | Corinna U. Keber³ |
 Andreas Kaufmann² | Ho-Ryun Chung⁴ | Emily P. Slater⁵ | Christopher Heeschen⁶ |
 Rita T. Lawlor⁷ | Aldo Scarpa⁷ | Detlef K. Bartsch⁵ | Thomas M. Gress¹ |
 Stefan Bauer² | Malte Buchholz^{1,8}

¹Clinic for Gastroenterology, Endocrinology, Metabolism and Infectiology, Philipps-University Marburg, Marburg, Germany

²Institute for Immunology, Philipps-University Marburg, Marburg, Germany

³Institute of Pathology, Philipps-University Marburg, Marburg, Germany

⁴Institute for Medical Bioinformatics and Biostatistics, Philipps-University Marburg, Marburg, Germany

⁵Department of Visceral, Thoracic and Vascular Surgery, Philipps University Marburg, Marburg, Germany

⁶Pancreatic Cancer Heterogeneity Group, Candiolo Cancer Institute, Candiolo (Torino), Italy

⁷ARC-Net Cancer Research Centre, University of Verona, Verona, Italy

⁸Core facility Small Animal Imaging of the Medical Faculty of the Philipps-University Marburg, Marburg, Germany

Correspondence

Malte Buchholz, Clinic for Gastroenterology, Endocrinology, Metabolism and Infectiology, Philipps-University Marburg, H103 Zentrum für Tumor- und Immunbiologie (ZTI), Hans-Meerwein Straße 3, 35043 Marburg, Germany.
 Email: malte.buchholz@staff.uni-marburg.de

Funding information

Deutsche Forschungsgemeinschaft, Grant/Award Number: DFG-KFO325

Abstract

Background: Toll-like receptors (TLRs) are gaining attention for their potential to influence tumor biology both on the level of the tumor cells as well as on the level of the surrounding inflammatory stroma. Previous studies resulted in partly conflicting data on the expression of TLR7 in healthy and neoplastic pancreatic tissues as well as its role in pancreatic tumor biology.

Methods: We used qRT-PCR and immunohistochemistry to assess TLR7 expression in primary patient material and cell lines. Cell viability was analyzed by MTT assay upon incubation with TLR7 agonist/antagonist. Mouse models were used to investigate the role of TLR7 in vivo.

Results: TLR7 is overexpressed in more than 50% of primary human pancreatic ductal adenocarcinoma (PDAC). High TLR7 expression was associated with shorter patient survival, and TLR7 inhibition in cell lines reduced viability in a dose-dependent manner. In contrast, global TLR7 deficiency did not alter survival or overall histopathological tumor features in genetic mouse models of PDAC.

Conclusions: TLR7 may have opposing functions in tumor versus stroma cells. Further work is required to more precisely dissect the roles of TLR7 and its

Maren Stark, Marina Nicolai and Marina Tatura contributed equally and should be considered joint first authors. Thomas M. Gress, Stefan Bauer, and Malte Buchholz contributed equally and should be considered joint last authors.

This is an open access article under the terms of the [Creative Commons Attribution](https://creativecommons.org/licenses/by/4.0/) License, which permits use, distribution and reproduction in any medium, provided the original work is properly cited.

© 2023 The Authors. *Cancer Medicine* published by John Wiley & Sons Ltd.

ligands in different populations of epithelial and stromal cells and to understand their relative contributions to tumor progression.

1 | BACKGROUND

Pancreatic ductal adenocarcinoma (PDAC) exhibits the worst prognosis among all solid tumors with a median survival of 6 months.¹ Early diagnosis is rare due to the relatively unspecific clinical symptoms, such as back pain, loss of appetite, or weight.² Definite diagnosis is reached by endoscopic ultrasound, computed tomography, or magnetic resonance imaging.³ Systemic chemotherapy is currently the only treatment for patients with advanced, metastatic PDAC and therefore new therapies such as efficient immunotherapy are urgently needed. Unfortunately, effective immunotherapy responses in PDAC are rare due to immunosuppressive tumor microenvironment mediated, among others, by myeloid suppressor cells. Therefore, modification of the immune landscape of these tumors by activation or inhibition of innate or adaptive immune pathways may be a promising strategy.

Pattern recognition receptors (PRRs) function in the innate immune system to sense pathogen-derived molecules and to initiate an appropriate immune response. Nucleic acid from bacteria and viruses are prominent target structures that are recognized by cytoplasmic or endosomal/lysosomal PRRs with subsequent cytokine production and cellular activation, but the evidence is mounting that PRRs can also be activated by endogenous molecules.⁴ In the cytoplasm, cGAS or RIG-I-like receptors (RLH) recognize DNA or RNA, respectively. RIG-I senses 5'-triphosphorylated RNA from viral and bacterial RNA or endogenous RNA fragments generated by RNase digestion.⁵ In the endosomal/lysosomal compartment Toll-like receptors TLR7 and TLR8 sense RNA⁶⁻⁸ in form of degradation products,^{9,10} whereas TLR9 is activated by DNA with CpG sequence motif.¹¹⁻¹³

Of note, most of these PRRs are highly expressed in macrophages, including tumor-associated macrophages (TAMs), which play an integral part in shaping the tumor microenvironment. Among others, TAMs have been shown to be supportive of cancer growth, invasion, and metastasis,¹⁴ to be involved in establishing local T-cell immune privilege,¹⁵ and to mediate resistance to radiotherapy in PDAC.¹⁶ Interestingly, systemic depletion of macrophages significantly diminished metastasis formation in genetically engineered mouse models of PDAC.¹⁷ However, PRRs are not only expressed by immune cells but also by cancer cells as well as stroma cells, thus having the potential to influence tumor biology, including therapy resistance, on multiple levels. For example, activated

RIG-I-like helicases induce immunogenic cell death of pancreatic cancer cells and sensitize tumors toward killing by CD8⁺ T cells.¹⁸ In addition, TLR9 activation improves the response to radiofrequency ablation therapy in a rabbit liver cancer model.¹⁹ In contrast, TLR9 as well as TLR7 have initially been described to exert tumor-promoting roles in pancreatic cancer: TLR9 ligation was demonstrated to induce pancreatic stellate cells (PSCs) to become fibrogenic and secrete chemokines that promote epithelial cell proliferation,²⁰ and stimulation of TLR7 was shown to lead to an acceleration of tumor progression, while its inhibition attenuated cancer cell growth in vitro as well as in mouse models.²¹ In contrast, using syngeneic orthotopic murine tumor models, Michaelis et al. demonstrated, that treatment of tumor-bearing mice with the TLR7/8 agonist R848 reduced tumor mass and improved survival.²²

Here, we show that TLR7 is expressed and activated in pancreatic cancer cells in vitro and in vivo and promotes the proliferation of tumor cells. Moreover, high TLR7 expression in primary human tumor tissue samples was associated with significantly shortened survival. In contrast, global knockout of TLR7 expression in the well-established KPC mouse model of pancreatic cancer did not result in attenuated tumor progression or increased survival of the mice. Our results thus support the notion that globally, TLR7 has no exclusive tumor-promoting or tumor-suppressive functions in PDAC.

2 | METHODS

2.1 | Patients, cell lines, and short-term cell cultures

The human pancreatic adenocarcinoma cell lines Panc1, PaTu-8988 T, and S2-007 were used in this study. Panc-1 cells and THP-1 monocytes were obtained from the American Type Culture Collection. S2-007 cells were from T. Iwamura²³ (Miyazaki Medical College). PaTu-8988 T cells were kindly provided by H. P. Elsässer (Cytobiology and Cytopathology Institute, Philipps University).

Short-term cultures of pancreatic cancer cells from KC mice (KC623) as well as from human circulating PDAC stem cells (Lon556 and Lon560) were established as previously described.²⁴

Lon556 and Lon560 were cultured in RPMI 1640 medium supplemented with 10% FCS and 0.05 mg/mL Gentamicin, the other cell lines were cultured in

Dulbecco's modified eagle medium (DMEM) containing 5% FCS at 37°C and 5% (v/v) CO₂.

Written informed consent was obtained from all patients prior to using tissue samples and Ethics Committee approval was available at all sites. The study was approved by the Ethics Committees at the University of Marburg and the University of Verona.

2.2 | Construction of tissue microarrays

For the construction of tissue microarrays (TMAs), 1.0 mm sized tissue biopsies were extracted from paraffin donor blocks and transferred into pre-punched holes on recipient paraffin blocks with a tissue microarrayer (Beecher Instruments, Inc.) equipped with a TMA booster (Alphelys). Grid layouts for tumor and normal pancreatic tissue TMAs were designed with the TMA Designer 2 software (Alphelys). The recipient blocks were sealed for 10 min at 56°C and 30 min at 4°C. This procedure was repeated twice. The TMA blocks were cut into 3.5 μm sections and placed on SuperFrost Plus slides for immunohistochemical staining.

2.3 | Histology and immunohistochemistry

For immunohistochemistry, heat-induced epitope retrieval was performed with citrate buffer. Staining was performed on a DAKO autostainer plus. After blocking endogenous peroxidase, sections were incubated for 45 minutes with rabbit polyclonal Anti-TLR7 antibody (1:50; Proteintech #17232-1-AP) or anti-CD68 antibody (1:100; Dako #MO876), respectively. Sections were washed and incubated with Dako REAL EnVision HRP Rabbit/Mouse polymer, which reacts with DAB-Chromogen, according to the manufacturer's protocol. Histology and staining results were evaluated in a blinded fashion by an experienced pathologist (C. Keber). Only cases where at least 2 independent biopsy cores could be evaluated were counted. Staining intensity was graded on a scale from 0 to 3 (absent, weak, moderate, strong), and a mean score was calculated for each patient.

2.4 | Primers, agonist, antagonist

For expression analysis following primers were used:

TLR7_h/m: FW: 5'-CCCAGAAAATGTCCTCAACAA-3'; RV: 5'-ATGGTTAACCCACCAGACAAA-3'.

RPLP0_h/m:FW: 5'-TGGGCAAGAACACCATGATG-3'; RV: 5'-AGTTTCTCCAGAGCTGGGTTGT-3' (both primer pairs detect human and mouse transcripts simultaneously).

For TLR7 activation/inactivation the following agonist/antagonist was used: TLR7 agonist CL264 (9-benzyl-8-hydroxyadenine derivative containing a glycine on the benzyl group (in para); InvivoGen, cat: # tlrl-c264e), TLR7(9) antagonist IRS-954 (immunoregulatory sequence; TIB Molbiol): 5'-TGCTCCTGGAGGGTTGT-3', unspecific control oligo Ctr_ODN (TIB Molbiol): 5'-TCCTGCAGGTTAAGT-3'.

2.5 | Treatment with TLR7 agonist/antagonist

The different cell lines were seeded onto 6 well plates in different cell numbers depending on their cell growth (LON560: 90.000/well; KC623: 75.000/well; S2-007: 30.000/well). KC623 cells were treated on the following day, LON560 2 days after seeding and S2-007 was pre-incubated 1 day in a serum-free medium before treatment was added. On the day of the treatment, the cells were washed once with PBS, the medium was changed to medium with reduced serum concentration (0% or 1% serum as indicated in the respective figure), and CL264 or IRS-954/Ctr_ODN was added.

2.6 | Cell viability assays

Cell viability was measured by MTT assay as described previously.^{25,26} Briefly, after 72 h of incubation, cells were incubated for 1–2 h with MTT-reagent (thiazolyl blue, Carl Roth GmbH) at 37°C, solubilized and measured at 570 nm with the Multiskan FC photometer (Thermo Scientific).

2.7 | Protein extraction and Western Blot analyses

The following antibodies were used for western blot analyses: anti-Cyclin D1 (Abcam, cat. # ab16663); anti-p21 (Cell Signaling, cat. # 2947); anti-PARP (Cell Signaling, cat. # 9532); anti-caspase-3 (Cell Signaling, cat. # 9664 and 9665); anti-actin, HRP coupled (Sigma-Aldrich, cat. # A3854); anti-TLR7 (Proteintech cat. #17232-1-AP).

For protein extraction, cells were collected together with medium and centrifuged at 1600 rpm at 4°C for 5 minutes. Pellets were washed twice with ice-cold PBS and then re-suspended in 200 ml lysis buffer (PBS containing protease inhibitors (Protease Arrest, GBiosciences) and phosphatase inhibitors (PMSF 1 mmol/L, EDTA 0.5 mmol/L, sodium pyrophosphate 25 mmol/L, sodium orthovanadate, 10 mmol/L, sodium fluoride 50 mmol/L)). Cells were sonicated (LabSonic, BBraun) and protein content was

assessed using Protein Assay Reagent (Thermo Scientific). For Western blotting, 15 mg proteins were electrophoresed on SDS-polyacrylamide gels and electrophoretically transferred onto nitrocellulose membranes (Optitran, GE Healthcare Life Sciences). Membranes were blocked in 5% nonfat dry milk in TBST (10 mmol/L Tris-HCl, pH 7.6, 100 mmol/L NaCl, 0.1% Tween 20) for 2 hours at room temperature and then probed with appropriate antibodies.

2.8 | Animal experiments

Mice were maintained in IVCs in a climate-controlled room kept at 22°C, exposed to a 12:12-hour light-dark cycle, fed standard laboratory chow, and given water ad libitum.

The *TLR7*^{-/-} mouse strain as well as the *LsL-Kras*^{G12D}; *Pdx1-Cre* double mutant (“KC mice”) and *LsL-Kras*^{G12D}; *LsL-Trp53*^{R172H}; *Pdx1-Cre* triple mutant (“KPC mice”) strains have been described previously.^{27,28} All mouse strains were originally on a mixed 129/SvJ/C57Bl/6 background but were backcrossed to a pure C57Bl/6 background for at least six generations. Mutant strains were intercrossed to produce cohorts with the genotypes indicated in the manuscript.

Upon signs of terminal illness, such as weight loss, diminished activity, and/or abdominal bloating due to ascites, mice were euthanized and the pancreas was removed, inspected for grossly visible tumors, and preserved in 4% formalin solution (Otto Fischer GmbH). All animals that were found to have invasive adenocarcinomas of the pancreas upon necropsy were included as events. Animals that died of other causes, as determined by histologic evaluation of pancreata after necropsy, as well as animals that were still alive at the time of evaluation, were censored.

All animal procedures were ethically reviewed and approved by Regierungspräsidium Gießen (Germany) and all experiments were performed in accordance with the European guidelines for the care and use of laboratory animals confirming Directive 2010/63/EU.

2.9 | GO enrichment analysis of tumor material from KPC mice

Whole transcriptome sequencing was performed on FFPE (formalin-fixed paraffin-embedded) tissue from WT KPC ($n = 9$) and *TLR7*^{-/-} KPC ($n = 10$) pancreata by a commercial service (CeGaT GmbH, Tübingen, Germany) and reads mapped to a standard genome.²⁹ Normalized read counts were used to identify differentially expressed genes using a 10% false discovery rate as a threshold, and the resulting list was analyzed for significantly enriched gene

sets using the PANTHER Classification System (pantherdb.org)³⁰.

2.10 | Software

To compute and compare survival rates between mouse cohorts as well as to analyze patient clinicopathological data and generate Kaplan–Meier curves, the GraphPad Prism 9 program (GraphPad Software) was used.

3 | RESULTS

3.1 | TLR7 is expressed in human pancreatic cancer cells in vivo and in vitro

Staining of tissue microarray (TMA) sections of human primary cases of PDAC ($n = 52$) with TLR7-specific antibodies revealed that TLR7 is strongly overexpressed in 23% ($n = 12$) and weakly/moderately expressed in 77% ($n = 40$) of cases (Figure 1B,D & E). Staining of normal exocrine tissue was uniformly weak (Figure 1A & C), while normal pancreatic islets showed moderate staining intensities (Figure 1A). A comparison of clinicopathological features with TLR7 expression data revealed no statistically significant correlation of TLR7 expression status with tumor grade, stage, or TNM status (Table 1). However, high TLR7 expression in the tumor correlated with statistically significantly reduced overall survival (Figure 2A) with all long-time survivors (>36 months after diagnosis) showing weak to moderate TLR7 expression (Figure 2B).

Quantitative real-time PCR analyses showed that TLR7 was highly expressed at the mRNA level in short-term cultures from both, human (LON560) as well as murine (KC623) PDAC tumor cells. In contrast, expression was low or absent in established long-term cultured cell lines derived both from liver metastases (PaTu-8988 T, S2-007) as well as from primary tumors (Panc-1) (Figure 2C). For verification real-time PCR analysis was repeated in the presence of TLR7-positive THP-1 monocytic cells (Figure S1A).

3.2 | Inhibition of TLR7 reduces cell viability in vitro

To investigate the functional role of TLR7 expression in pancreatic cancer cells, we treated TLR7-high human Lon560 and murine KC623 cells with the well-established inhibitor IRS-954. Inhibition of TLR7 led to strongly reduced cell viability in LON560 cells (Figure 3A, left panel). This effect was less pronounced, but also clearly apparent

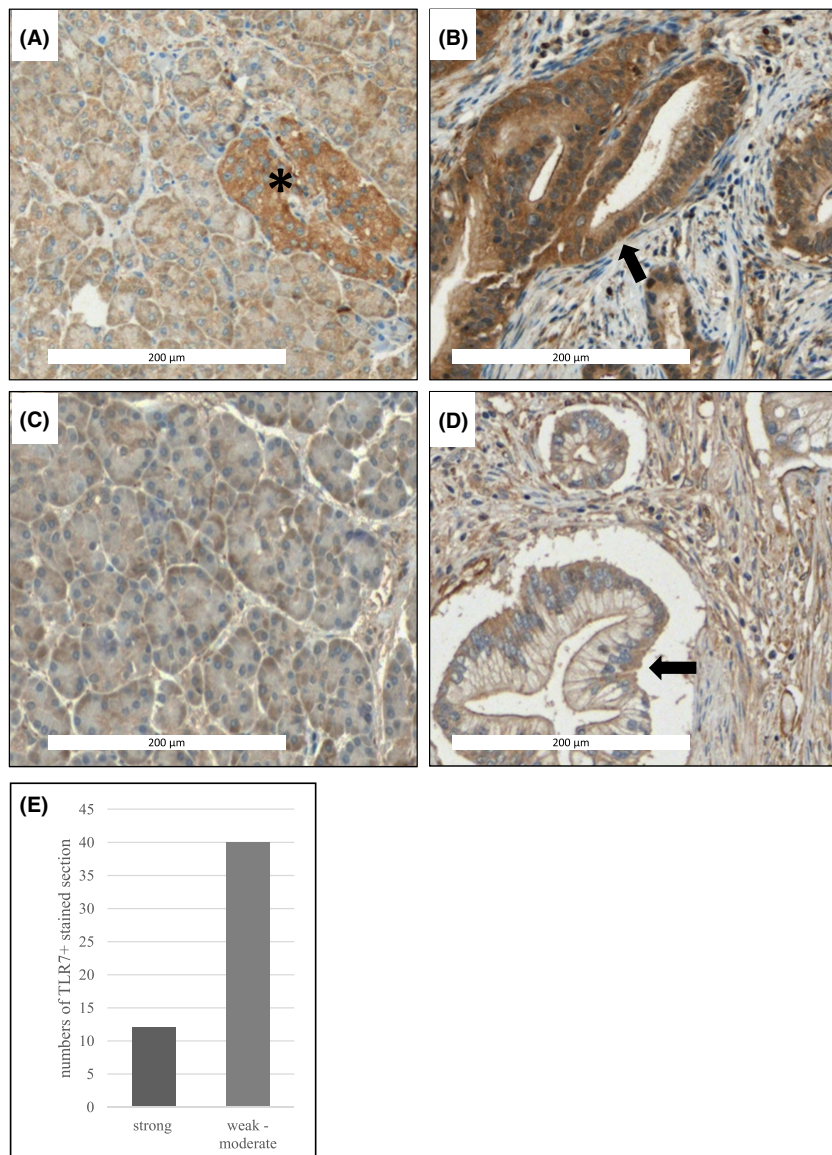


FIGURE 1 Expression of TLR7 in primary human tissues. (A–D) Tissue microarrays (TMAs) of human PDAC (B, D) and corresponding normal (A, C) tissue, were stained against TLR7 (Proteintech #17232-1-AP), results showing strong (B) and moderate (D) expression of TLR7 in tumor cells (arrows). Islets of Langerhans (A, asterisk) also stained positive for TLR7. E: Quantification of staining results from TMA sections.

in KC623 cells (Figure 3B, left panel). Conversely, treatment of the TLR7-low S2-007 cells with the same inhibitor at a high dose showed only a mild impact on cell viability (Figure 3C). Functionally, inhibition of TLR7 through IRS-954 did not lead to reduced mRNA levels neither in cancer cells nor in THP-1 monocytic control cells (Figure S1B).

Interestingly, treatment with the TLR7 agonist CL264 had little or no effect on LON560 cells even in the absence of any other potential stimulants (serum-free culture conditions) (Figure 3A, right panel), suggesting that TLR7 activity was already maximally stimulated by endogenous ligands in these cells. KC623 cells showed moderate growth-stimulatory effects after CL264 treatment (Figure 3B, right panel), correlating with the less pronounced growth inhibition by the IRS-954 inhibitor.

In order to test whether reduced viability was due to the induction of apoptosis or activation of classical cell cycle checkpoints, we performed Western blot analyses

of typical markers for both processes. However, neither PARP nor Caspase-3 cleavage as markers of apoptosis induction, nor regulation of cell growth-associated proteins Cyclin D1 and p21 as typical markers of cell cycle arrest were apparent following TLR7-inhibition, suggesting that reduced viability is the consequence of more complex regulatory mechanisms (Figure S2).

3.3 | Global TLR7 deficiency does not attenuate tumor progression in transgenic mouse models of pancreatic cancer

In order to evaluate the dependency of pancreatic tumorigenesis on TLR7 expression *in vivo*, we crossed mice with a global TLR7 knockout (TLR7^{-/-} mice) with mice of the KC and KPC strains. As shown in Figure 4A, TLR7 status did not have any discernable influence on the survival

TABLE 1 Summary of clinicopathological data of primary human PDAC tissue donors. From originally 76 cases, 62 cases with at least 2 out of 3 TMA sections available were analyzed. Of these 10 cases were classified as intraductal papillary mucinous neoplasm (IPMN) and therefore excluded from analyses. The remaining cases were categorized into two groups, depending on the mean TLR7 staining intensity of the respective sections (weak to moderate or strong). The distribution of parameters was analyzed by Chi² Test of Trend showing no significant differences between groups

| Variable | Cases | TLR7 expression | | p-value | | |
|-----------------------|-------|-------------------|--------|---------|------|------|
| | | weak/ moderate | strong | | | |
| TLR7 staining | 52 | 40 | 77% | 12 | 23% | |
| Clinical Stage (AJCC) | 45 | 35 | | 10 | | |
| IA | 1 | 1 | 100% | 0 | 0% | 0.83 |
| IB | 14 | 10 | 71% | 4 | 29% | |
| IIA | 7 | 6 | 86% | 1 | 14% | |
| IIB | 23 | 18 | 78% | 5 | 22% | |
| Tumor Size | 47 | 36 | | 11 | | 0.59 |
| <2 cm | 4 | 4 | 100% | 0 | 0% | |
| 2–4 cm | 30 | 22 | 73% | 8 | 27% | |
| >4 cm | 13 | 10 | 77% | 3 | 23% | |
| Tumor Grade | 45 | 35 | | 10 | | 0.87 |
| G1 | 1 | 1 | 100% | 0 | 0% | |
| G2 | 36 | 27 | 75% | 9 | 25% | |
| G3 | 7 | 7 | 100% | 0 | 0% | |
| G4 | 1 | 0 | 0% | 1 | 100% | |
| % of cases showing | 42 | 33 | | 9 | | |
| Lymphatic invasion | 6 | 5 | 83% | 1 | 17% | |
| Vascular invasion | 5 | 4 | 80% | 1 | 20% | |
| Perineural invasion | 28 | 21 | 75% | 7 | 25% | |

of KPC mice, with a median survival of 171 days in the TLR7^{-/-} cohort compared to 198 days in KPC WT mice. In the less severe KC tumor mouse model, TLR7^{-/-} KC mice even tended to display a trend to shorter survival (Figure 4A), although it should be noted that many animals from this cohort had to be sacrificed for reasons unrelated to pancreatic tumorigenesis (mainly development of papillomas and lymphomas), which may be attributable to impaired restriction of endogenous retrovirus (ERV) activation as previously reported for TLR7^{-/-} mice.³¹

Blinded evaluation of histological features of end-stage tumors from KPC mice demonstrated considerable inter-tumoral heterogeneity in features such as tumor cell differentiation, stroma content, or lymphocyte infiltration, but did not reveal systematic differences between

tumors from TLR7^{-/-} or TLR7^{wt} KPC mice (Figure 4B, C). Likewise, there was no systematic difference in the presence of monocytic cells in TLR7^{-/-} or TLR7^{wt} KPC tumors as evaluated by CD68 staining of representative tumor sections (Figure 4D, E).

In an effort to gain further insights into potential systematic changes on the RNA level, we performed RNAseq analysis of bulk tumor material from TLR7^{-/-} ($n = 10$) and TLR7^{wt} ($n = 9$) KPC mice (Figure 5). Statistical analyses revealed a relatively small number of significantly differentially expressed genes ($n = 99$ at 10% false discovery rate; Table 2), which may again be reflective of relatively large intertumoral heterogeneity within both cohorts. Interestingly, however, gene set enrichment analysis of the sequencing data using the PANTHER Classification System revealed that a large number of GO terms related to immune system functions, such as “leukocyte activation (GO:0045321),” “lymphocyte activation (GO:0046649),” “positive regulation of innate immune response (GO:0045089)” etc, which were significantly enriched among the set of regulated genes (Table 3), hinting at systematic changes in the immune landscape of the tumors in response to the TLR7 deficiency.

4 | DISCUSSION

In the course of developing immunotherapeutic approaches for the treatment of malignant tumors, TLR agonists are already used in clinical settings to induce anti-tumor immunity.^{32–35} In this context, TLRs have also been proposed as potential targets in the therapy of PDAC, but studies addressing the biology and clinical utility of TLRs in general and TLR7, in particular, remain scarce.

Previous studies resulted in conflicting reports regarding the expression pattern of TLR7 in normal and neoplastic human pancreas tissue. While Ochi et al. reported that expression was completely absent from healthy pancreas but strongly present in both epithelial as well as stromal cells in PDAC,²¹ Helminen et al. described the distinct expression of TLR7 (as well as TLR8) in beta cells within pancreatic islets.³⁶ Our own results confirm the data of Helminen et al., clearly showing robust expression of TLR7 in islets of Langerhans. This result can be taken as further evidence of the fact that the role of pattern recognition receptors extends beyond their functions in the innate immune system, both in physiological as well as pathophysiological contexts.

Our data further confirm that TLR7 is expressed by tumor cells within primary human tumor tissue^{21,22,37} and high TLR7 expression seems to correlate with shorter overall survival which, to our knowledge, has

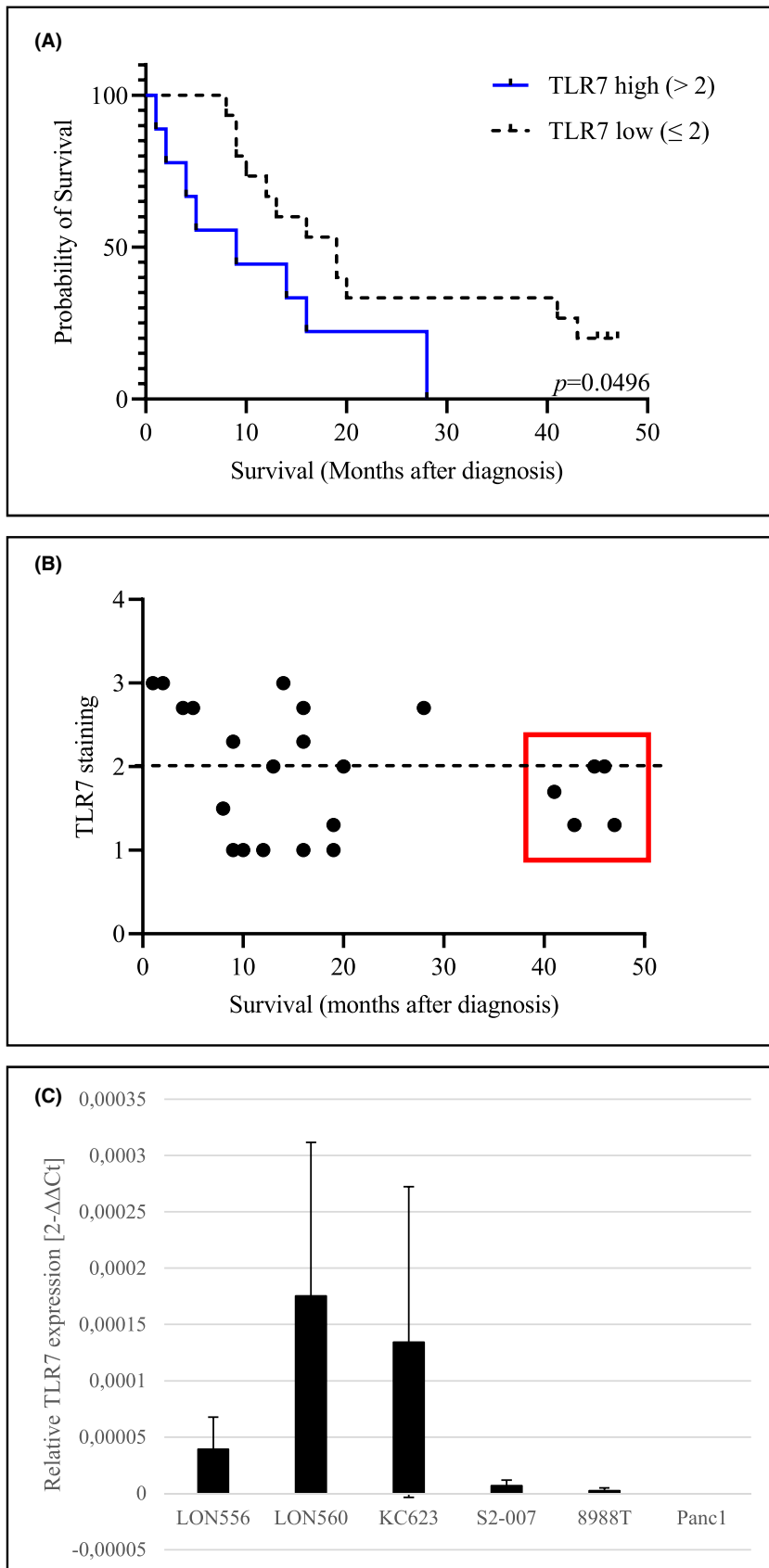


FIGURE 2 Correlation of TLR7 expression with patient survival and relative age of cell cultures. (A) Kaplan-Meier curves of overall survival according to TLR7 IHC (censored data are flagged). $n = 24$; Log-rank (Mantel-Cox) test. (B) Correlation of survival and TLR7 expression reveals that all long-time survivors (<36 months from diagnosis) exhibit weak to moderate TLR7 staining. (C) Q-RT-PCR analyses of TLR7 mRNA expression in short-term cultures upon thawing in comparison to established PDAC cell lines. Expression values are shown relative to the housekeeping gene RPLP0 in each cell line. Bars represent the mean \pm SDM of two to five independent experiments.

not been reported before. Although we could not observe any correlation between tumor stage and TLR7 expression as Grimmig et al. reported, analyses of our

clinicopathological data uncovered a group of long-time surviving patients showing exclusively weak to moderate TLR7 expression.

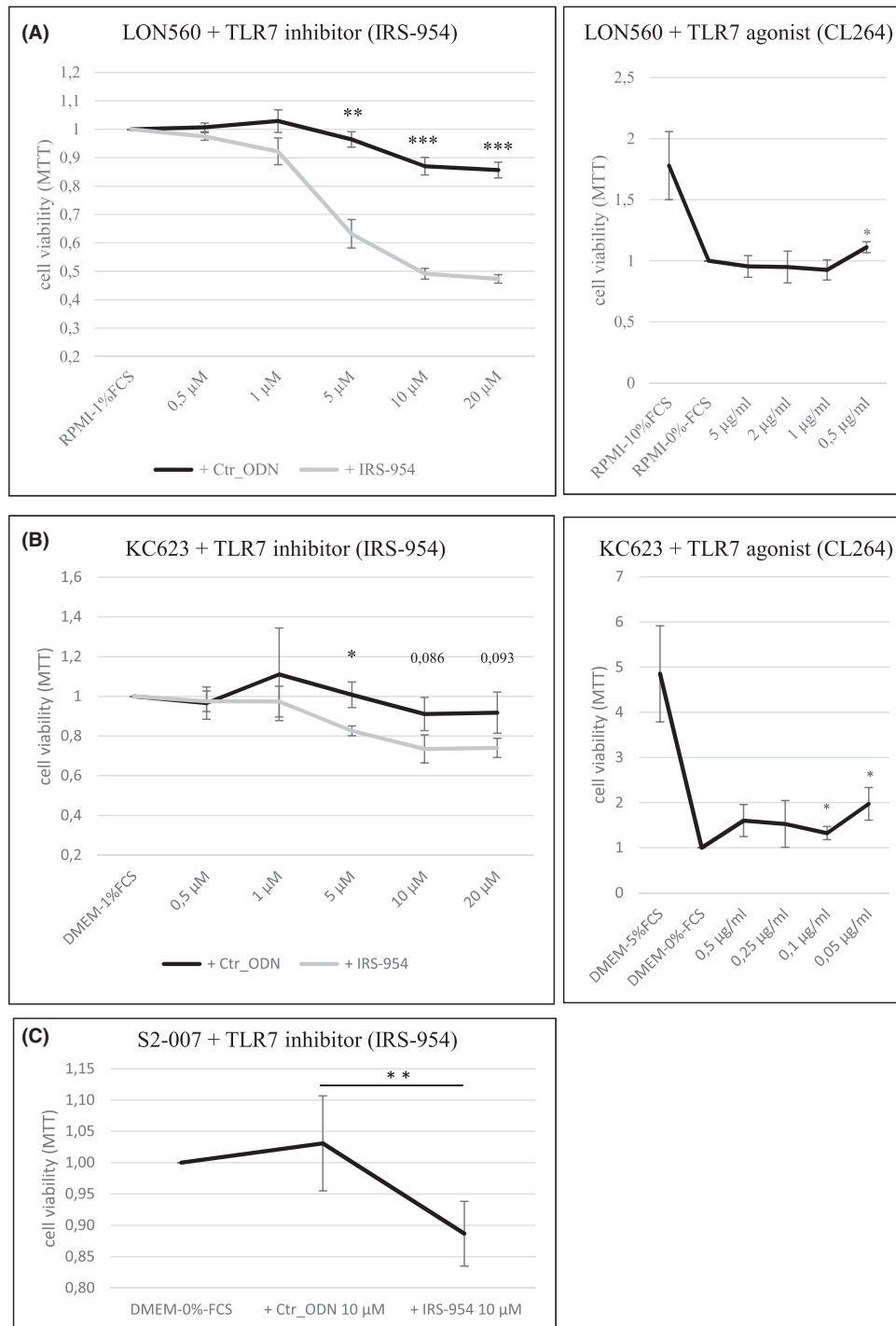


FIGURE 3 TLR7 mediates growth-stimulatory effects in cancer cells in vitro. (A & B) LON560 (A) and KC623 (B) were treated with different concentrations of IRS-954/Ctr_ODN [0.5 μ M–20 μ M] or CL264 [5 μ g/mL–0.5 μ g/mL or 0.5 μ g/mL–0.05 μ g/mL]. Cell viability was measured by MTT assay 72 h after treatment. (C) S2-007, a low-expressing TLR7 cell line, was treated with 10 μ M IRS-954/Ctr_ODN (concentration with the highest effect in LON560). Cell viability was measured by MTT assay 72 h after treatment. Bars represent the mean \pm SDM of at least three independent experiments normalized to control cells (0%-FCS/ 1%-FCS). Ctr_ODN, control oligo. (Students *t* test: **p* < 0.05, ***p* < 0.01, ****p* < 0.001).

In the course of this study, we further identified a subset of TLR7 expressing pancreatic cancer cell lines. Interestingly, short-term cultured cells from both human as well as mouse tumors showed considerably

higher TLR7 expression than high-passage established cell lines, indicating that TLR7 expression is not selected for under standard culture conditions and may be lost over time. Stimulation of TLR7-positive cells

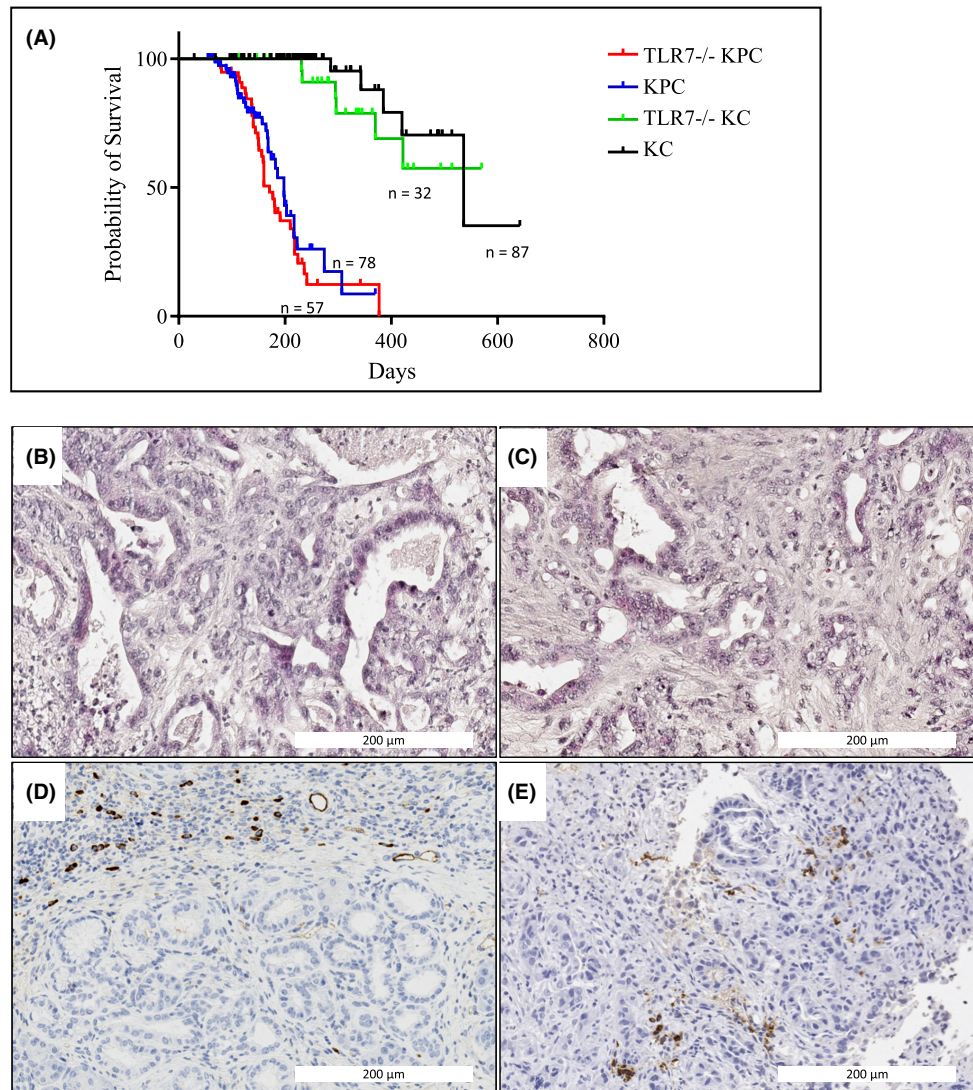


FIGURE 4 Global TLR7 knockout does not attenuate tumor progression in vivo. (A) Kaplan–Meier analyses revealed that TLR7 deficiency did not result in any survival benefit, neither in the KPC nor in the KC mouse model. (B & C) Representative histological sections (H&E staining) of 7-month-old WT-KPC (B) and TLR7^{-/-}-KPC (C) mice. (D & E) Representative images of CD68 staining for monocytes in 7-month-old WT-KPC (D) and TLR7^{-/-}-KPC (E) mice.

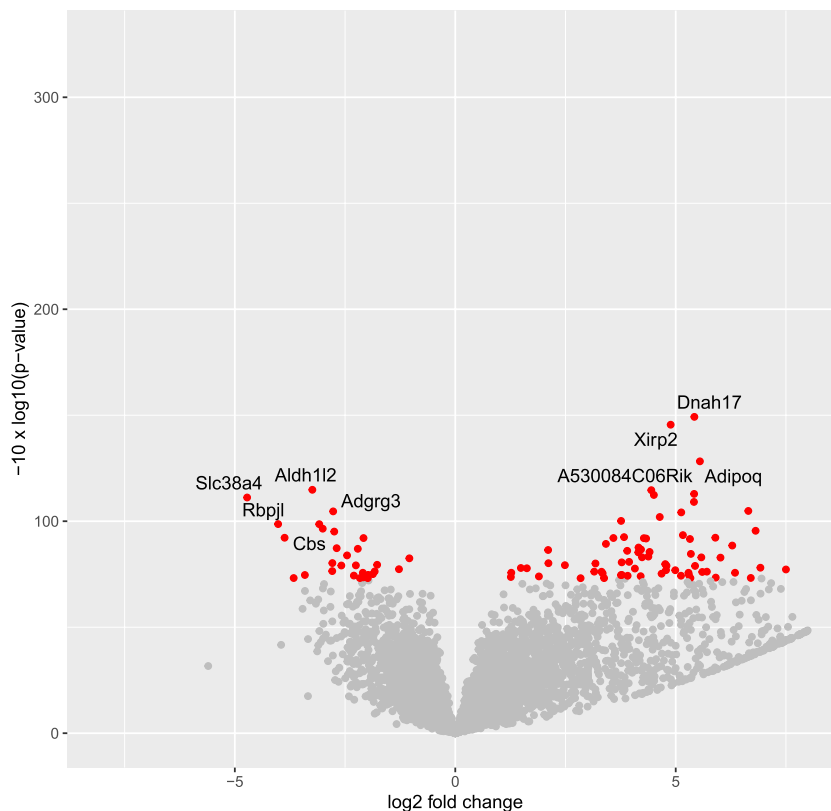
with a TLR7-specific agonist did not significantly alter cell growth, which is consistent with previous results showing that TLR7 ligation with ssRNA40 did not have any direct proliferative effects on transformed epithelial cells from KC mice and did not affect their viability.²¹ Conversely, inhibition of TLR7 in the same cell lines reduced cell viability in a dose-dependent manner, indicating that TLR7 is not only expressed and functional in the tumor cells but also active, which hints at the presence of effective endogenous ligands and autocrine signaling mechanisms.

Two studies have previously investigated the role of TLR7 in promoting or inhibiting pancreatic tumor progression in vivo, reporting partly conflicting results. The first one²¹ reported that treatment of p48Cre; Kras^{G12D}

(KC) mice with the TLR7 agonist ssRNA40 strongly accelerated tumor progression, while TLR7 inhibition with IRS-954 was able to block caerulein-induced inflammation-mediated tumor progression in KC mice. Effects of TLR7 inhibition on the natural course of disease (unstimulated by caerulein-induced inflammation) in KC or KPC mice were not reported.

In contrast, the second study²² reported that the TLR7 agonist R848 elicited strong anti-tumor responses in syngeneic orthotopic murine PDAC models and protected the animals from cachexia manifestations. The authors concluded that anti-tumor effects of R848 were mediated by host-derived TLR7-positive stromal cells, rather than by direct influence on neoplastic cells since the implantation of syngeneic tumor cells

FIGURE 5 Volcano plot of differentially expressed genes. The \log_2 FC (fold change) indicates the mean expression level for each gene. Positive values denote genes upregulated in TLR7 KO vs. control KPC tumors; negative values denote genes downregulated in TLR7 KO tumors. Each dot represents one gene; red dots denote genes significantly differentially expressed at a false discovery rate (FDR) of 10%.



in TLR7^{-/-} host mice with subsequent R848 treatment did not result in attenuated, but instead in accelerated tumor growth.

Of note, although both studies made use of the KC, KPC, and TLR7^{-/-} mouse strains also used in our study, neither study reported crossing the KC and/or KPC mouse model(s) onto the TLR7 knockout background. Instead, results were obtained by different combinations of a tumor cell or bone marrow cell grafting and treatment with TLR7 agonists or inhibitors. It is thus difficult to determine how faithfully either of these studies reflected the *in vivo* situation of pancreatic tumorigenesis, and in how far off-target effects or the pharmacodynamic properties of agonists and inhibitors influenced the study results. Our own results surprisingly demonstrated neither a protective nor a tumor-promoting net effect of TLR7 ablation *in vivo*, although tumor-promoting functions *in vitro* were readily apparent. This may be reflective of opposing roles of TLR7 functions in tumor cells versus cells of the inflammatory stroma, as can also be concluded from the observation of Michaelis et al. that tumor-attenuating effects of TLR7 agonist treatment were lost in TLR7^{-/-} mice and instead resulted in increased growth of TLR7-competent tumor cells in TLR7-deficient host animals.²² Our RNAseq analyses

indicate that despite considerable inter-tumoral heterogeneity in the KPC mouse model, TLR7 deficiency systematically alters the immune landscape in PDAC tumors. For instance, several genes known to play central roles in T cell biology, including transcription factors GATA3, Foxp3, and AIRE as well as the Interleukin12 receptor beta2, but also the B- And T-Lymphocyte Attenuator BTLA were significantly upregulated in TLR7^{-/-} tumors. On the contrary, the B cell regulator ADRGRG3 as well as the transcription factor RBPJ, has been shown to be a critical factor in T-helper (TH) subset polarization (<https://doi.org/10.1038/s41467-019-09276-w>), were found to be strongly downregulated in TLR7^{-/-} tumors. Of note is also the upregulation of the TLR1 receptor in response to the absence of TLR7 expression, although TLR1 and TLR7 sense very different sets of biomolecules. The profound impact of TLR7 deficiency on the immune landscape of pancreatic tumors is also reflected by the results of our gene set enrichment analyses which revealed that a large number of GO terms related to immune system functions, such as “leukocyte activation (GO:0045321),” “lymphocyte activation (GO:0046649),” “positive regulation of innate immune response (GO:0045089),” were significantly overrepresented among the differentially regulated genes.

TABLE 2 List of differentially expressed genes. TLR7 knockout ($n = 10$) and control KPC tumors ($n = 9$) were subjected to RNAseq analysis and readcounts were determined using HTseq-count. Listed are genes that were statistically significantly differentially expressed at a false discovery rate (FDR) of 10%. Positive values denote genes upregulated in TLR7 KO versus control KPC tumors; negative values denote genes downregulated in TLR7 KO tumors

| Gene name | Description | log2 Fold Change | padj |
|-------------|---|------------------|----------|
| Vmn1r181 | Vomeronal 1 receptor 181 | 23.432 | 1.17E-10 |
| Xirp2 | Xin Actin-binding repeat containing 2 | 4.886 | 0.0024 |
| Dnah17 | Dynein, axonemal, heavy chain 17 | 5.423 | 0.0024 |
| Adipoq | Adiponectin, C1Q, and collagen domain containing | 5.549 | 0.0099 |
| Aldh1l2 | Aldehyde dehydrogenase 1 family, member L2 | -3.242 | 0.0243 |
| A530084C06R | RIKEN cDNA A530084C06 gene | 4.446 | 0.0243 |
| Snx22 | Sorting nexin 22 | 4.504 | 0.0243 |
| Ccdc63 | Coiled-coil domain containing 63 | 5.418 | 0.0243 |
| Slc38a4 | Solute carrier family 38, member 4 | -4.721 | 0.0244 |
| Samd15 | Sterile alpha motif domain containing 15 | 5.414 | 0.0270 |
| Adgrg3 | Adhesion G protein-coupled receptor G3 | -2.770 | 0.0340 |
| Ccdc106 | Coiled-coil domain containing 106 | 5.126 | 0.0340 |
| Majin | Membrane-anchored junction protein | 6.647 | 0.0340 |
| Rimklb | Ribosomal modification protein rimk-like family member B | 4.638 | 0.0393 |
| Fanci | Fanconi anemia, complementation group I | 3.761 | 0.0441 |
| Rbpjl | Recombination signal binding protein for immunoglobulin kappa J | -4.018 | 0.0454 |
| Cbs | Cystathionine beta-synthase | -3.085 | 0.0454 |
| Cfap54 | Cilia and flagella associated protein 54 | -3.007 | 0.0530 |
| Slc38a3 | Solute carrier family 38, member 3 | -3.871 | 0.0536 |
| Nr5a2 | Nuclear receptor subfamily 5, group A, member 2 | -2.745 | 0.0536 |

TABLE 2 (Continued)

| Gene name | Description | log2 Fold Change | padj |
|--------------|--|------------------|--------|
| Adgb | Androglobin | -2.081 | 0.0536 |
| C130026I21Ri | RIKEN cDNA C130026I21 gene | 3.587 | 0.0536 |
| Gm10718 | Predicted gene 10,718 | 3.828 | 0.0536 |
| Trpm3 | Transient receptor potential cation channel, subfamily M, member 3 | 4.277 | 0.0536 |
| Plin1 | Perilipin 1 | 4.329 | 0.0536 |
| Iqsec3 | IQ motif and Sec7 domain 3 | 5.163 | 0.0536 |
| Tmigd1 | Transmembrane and immunoglobulin domain containing 1 | 5.323 | 0.0536 |
| Cacna2d3 | Calcium channel, voltage-dependent, alpha2/delta subunit 3 | 5.899 | 0.0536 |
| Gm11127 | Predicted gene 11,127 | 6.812 | 0.0536 |
| Btla | B and T lymphocyte associated | 3.417 | 0.0652 |
| Ndp | Norrie disease (pseudoglioma) | 6.283 | 0.0682 |
| Cpn1 | Carboxypeptidase n, polypeptide 1 | -2.690 | 0.0725 |
| Zfp236 | Zinc finger protein 236 | -2.211 | 0.0725 |
| Gata3 | GATA binding protein 3 | 2.106 | 0.0725 |
| Abcc2 | ATP-binding cassette, subfamily C (CFTR/MRP), member 2 | 4.157 | 0.0725 |
| Gm10801 | Predicted gene 10,801 | 4.213 | 0.0725 |
| Olf639 | Olfactory receptor 639 | 3.900 | 0.0733 |
| Foxp3 | Forkhead box P3 | 4.152 | 0.0748 |
| Olf961 | Olfactory receptor 961 | 4.408 | 0.0748 |
| Aire | Autoimmune regulator | 5.344 | 0.0784 |
| Srrm4 | Serine/arginine repetitive matrix 4 | -2.454 | 0.0821 |
| Spock3 | Sparc/osteonectin, cwcv, and kazal-like domains proteoglycan 3 | 4.236 | 0.0831 |
| Scrt1 | Scratch family zinc finger 1 | 4.380 | 0.0831 |
| Ppp1r1c | Protein phosphatase 1, regulatory inhibitor subunit 1C | 5.581 | 0.0831 |
| Vmn1r197 | Vomeronal 1 receptor 197 | 6.015 | 0.0831 |
| Appl2 | Adaptor protein, phosphotyrosine interaction 2 | -1.041 | 0.0840 |
| Glt1d1 | Glycosyltransferase 1 domain containing 1 | -2.788 | 0.0953 |

TABLE 2 (Continued)

| Gene name | Description | log2 Fold Change | padj |
|-----------|--|------------------|--------|
| Ptpn2 | Protein tyrosine phosphatase, receptor type, N polypeptide 2 | -2.584 | 0.0953 |
| Wnk2 | WNK lysine deficient protein kinase 2 | -2.254 | 0.0953 |
| Gpt | glutamic pyruvic transaminase, soluble | -1.772 | 0.0953 |
| H2ax | H2A.X variant histone | 2.113 | 0.0953 |
| Chst1 | Carbohydrate sulfotransferase 1 | 2.487 | 0.0953 |
| Tlr1 | Toll-like receptor 1 | 3.180 | 0.0953 |
| Il12rb2 | Interleukin 12 receptor, beta 2 | 3.775 | 0.0953 |
| Rgs20 | Regulator of G-protein signaling 20 | 3.943 | 0.0953 |
| Gm11032 | Predicted gene 11,032 | 4.763 | 0.0953 |
| Trim66 | Tripartite motif-containing 66 | 4.791 | 0.0953 |
| M1ap | Meiosis 1-associated protein | 5.439 | 0.0953 |
| Pah | Phenylalanine hydroxylase | -3.665 | 0.0996 |
| Lrrc7 | Leucine-rich repeat containing 7 | -3.411 | 0.0996 |
| Adm2 | Adrenomedullin 2 | -2.791 | 0.0996 |
| Prox1 | prospero homeobox 1 | -2.300 | 0.0996 |
| Reps2 | RALBP1-associated Eps domain containing protein 2 | -2.163 | 0.0996 |
| Sox6 | SRY (sex-determining region Y)-box 6 | -2.097 | 0.0996 |
| Gls2 | Glutaminase 2 (liver, mitochondrial) | -2.086 | 0.0996 |
| Ipo11 | Importin 11 | -1.985 | 0.0996 |
| Unc5a | Unc-5 netrin receptor A | -1.976 | 0.0996 |
| Cntfr | Ciliary neurotrophic factor receptor | -1.868 | 0.0996 |
| Adk | Adenosine kinase | -1.828 | 0.0996 |
| Rora | RAR-related orphan receptor alpha | -1.277 | 0.0996 |
| Kcnd1 | Potassium voltage-gated channel, shal-related family, member 1 | 1.261 | 0.0996 |
| Ppp1r18 | Protein phosphatase 1, regulatory subunit 18 | 1.271 | 0.0996 |
| Sfxn3 | Sideroflexin 3 | 1.488 | 0.0996 |
| Pik3ip1 | phosphoinositide-3-kinase interacting protein 1 | 1.623 | 0.0996 |
| Irx3 | Iroquois-related homeobox 3 | 1.897 | 0.0996 |
| Rel2 | RELT-like 2 | 2.843 | 0.0996 |

TABLE 2 (Continued)

| Gene name | Description | log2 Fold Change | padj |
|-----------|---|------------------|--------|
| Catip | Ciliogenesis-associated TTC17 interacting protein | 3.152 | 0.0996 |
| Nanos1 | Nanos C2HC-type zinc finger 1 | 3.318 | 0.0996 |
| Rasd2 | RASD family, member 2 | 3.343 | 0.0996 |
| Cfd | Complement factor d (adipsin) | 3.376 | 0.0996 |
| Gm10800 | Predicted gene 10,800 | 3.759 | 0.0996 |
| Cpne9 | Copine family member ix | 3.777 | 0.0996 |
| Phex | Phosphate regulating endopeptidase homolog, x-linked | 3.910 | 0.0996 |
| Kcnb2 | Potassium voltage-gated channel, shab-related subfamily, member 2 | 4.074 | 0.0996 |
| Prss57 | Protease, serine 57 | 4.205 | 0.0996 |
| Pou3f1 | POU domain, class 3, transcription factor 1 | 4.680 | 0.0996 |
| Gm14226 | Predicted gene 14,226 | 4.780 | 0.0996 |
| Kcni4 | Kv channel interacting protein 4 | 4.990 | 0.0996 |
| Trhde | TRH-degrading enzyme | 5.120 | 0.0996 |
| Tex15 | Testis expressed gene 15 | 5.290 | 0.0996 |
| Ces1f | Carboxylesterase 1F | 5.299 | 0.0996 |
| Apoa1 | Apolipoprotein A-I | 5.333 | 0.0996 |
| Vmn1r60 | Vomer nasal 1 receptor 60 | 5.602 | 0.0996 |
| Gm10720 | Predicted gene 10,720 | 5.707 | 0.0996 |
| Slc6a19 | Solute carrier family 6 (neurotransmitter transporter), member 19 | 5.908 | 0.0996 |
| Myom2 | Myomesin 2 | 6.346 | 0.0996 |
| Olf1238 | Olfactory receptor 1238 | 6.703 | 0.0996 |
| Usp17la | Ubiquitin-specific peptidase 17-like A | 6.921 | 0.0996 |
| Gpr3711 | G protein-coupled receptor 37-like 1 | 7.500 | 0.0996 |

However, given the complex interplay of different types of immune and stroma cells in the tumor microenvironment and the wide range of subtypes and functional states of different immune cell populations, much more in-depth work will be required to precisely dissect the roles of TLR7 and its ligands in different populations of epithelial and stromal cells and to understand their relative contributions to the promotion or attenuation of tumor progression in pancreatic cancer.

TABLE 3 List of GO terms significantly enriched among differentially expressed genes. Differentially expressed genes (Table 2) were analyzed for significantly enriched gene sets using the PANTHER Classification System. Interestingly upregulated genes in TLR7 knockout tumors (+) clustered around immune system-related GO terms

| GO biological process complete | Regul. | p-value | fdr |
|--|--------|-----------|-----------|
| Chromatin organization involved in the regulation of transcription (GO:0034401) | + | 3.17 E-08 | 4.90 E-04 |
| DNA packaging (GO:0006323) | + | 4.94 E-07 | 3.81 E-03 |
| Leukocyte activation (GO:0045321) | + | 6.52 E-07 | 3.36 E-03 |
| Regulation of lymphocyte activation (GO:0051249) | + | 8.86 E-07 | 3.42 E-03 |
| Cell activation (GO:0001775) | + | 1.42 E-06 | 4.38 E-03 |
| Regulation of leukocyte activation (GO:0002694) | + | 2.29 E-06 | 5.89 E-03 |
| Regulation of cell activation (GO:0050865) | + | 3.32 E-06 | 7.32 E-03 |
| Immune system process (GO:0002376) | + | 4.00 E-06 | 7.72 E-03 |
| Positive regulation of gene expression, epigenetic (GO:0045815) | + | 4.49 E-06 | 7.70 E-03 |
| Lymphocyte activation (GO:0046649) | + | 5.23 E-06 | 8.07 E-03 |
| Regulation of immune system process (GO:0002682) | + | 5.38 E-06 | 7.54 E-03 |
| Translation (GO:0006412) | + | 7.39 E-06 | 9.51 E-03 |
| Chromatin organization involved in negative regulation of transcription (GO:0097549) | + | 7.58 E-06 | 8.99 E-03 |
| Cellular amino acid metabolic process (GO:0006520) | - | 8.07 E-06 | 8.89 E-03 |
| Chromatin assembly (GO:0031497) | + | 9.55 E-06 | 9.82 E-03 |
| Long-chain fatty acid metabolic process (GO:0001676) | + | 1.50 E-05 | 1.44 E-02 |
| Peptide biosynthetic process (GO:0043043) | + | 2.53 E-05 | 2.30 E-02 |
| Positive regulation of innate immune response (GO:0045089) | + | 2.64 E-05 | 2.26 E-02 |
| Olefinic compound metabolic process (GO:0120254) | + | 2.79 E-05 | 2.26 E-02 |
| Regulation of interferon-gamma production (GO:0032649) | + | 2.80 E-05 | 2.16 E-02 |
| Regulation of gene expression, epigenetic (GO:0040029) | + | 3.40 E-05 | 2.50 E-02 |
| Chromatin assembly or disassembly (GO:0006333) | + | 4.13 E-05 | 2.90 E-02 |
| Positive regulation of immune system process (GO:0002684) | + | 5.98 E-05 | 4.01 E-02 |

TABLE 3 (Continued)

| GO biological process complete | Regul. | p-value | fdr |
|---|--------|-----------|-----------|
| Selective autophagy (GO:0061912) | - | 6.09 E-05 | 3.92 E-02 |
| T Cell activation (GO:0042110) | + | 6.25 E-05 | 3.86 E-02 |
| Alpha-amino acid metabolic process (GO:1901605) | - | 7.00 E-05 | 4.15 E-02 |
| Regulation of lymphocyte proliferation (GO:0050670) | + | 8.00 E-05 | 4.57 E-02 |
| Regulation of mononuclear cell proliferation (GO:0032944) | + | 8.06 E-05 | 4.44 E-02 |

Abbreviations: fdr, false discovery rate; regul., regulation.

AUTHOR CONTRIBUTIONS

Maren Stark: Data curation (equal); formal analysis (equal); investigation (equal); visualization (equal); writing – original draft (equal). **Marina Nicolai:** Data curation (equal); formal analysis (equal); investigation (equal); visualization (equal); writing – original draft (equal); writing – review and editing (equal). **Marina Tatura:** Data curation (equal); formal analysis (equal); investigation (equal); visualization (equal); writing – original draft (equal); writing – review and editing (equal). **Corinna U. Keber:** Data curation (equal); formal analysis (equal); investigation (equal); visualization (equal); writing – review and editing (equal). **Andreas Kaufmann:** Data curation (equal); formal analysis (equal); investigation (equal); visualization (equal); writing – review and editing (equal). **Ho-Ryon Chung:** Formal analysis (equal); visualization (equal); writing – review and editing (equal). **Emily P. Slater:** Data curation (equal); investigation (equal); writing – review and editing (equal). **Christopher Heeschen:** Formal analysis (equal); visualization (equal); writing – review and editing (equal). **Rita T Lawlor:** Data curation (equal); formal analysis (equal); investigation (equal); visualization (equal); writing – review and editing (equal). **Aldo Scarpa:** Formal analysis (equal); visualization (equal); writing – review and editing (equal). **Detlef K. Bartsch:** Data curation (equal); funding acquisition (equal); investigation (equal); resources (equal); writing – review and editing (equal). **Thomas Gress:** Conceptualization (equal); funding acquisition (equal); resources (equal); supervision (equal); visualization (equal); writing – review and editing (equal). **Stefan Bauer:** Conceptualization (equal); formal analysis (equal); funding acquisition (equal); project administration (equal); resources (equal); supervision (equal); visualization (equal); writing – review and editing (equal). **Malte Buchholz:** Conceptualization (equal); formal analysis (equal); funding acquisition (equal); project administration (equal); resources (equal); supervision (equal); visualization (equal); writing – review and editing (equal).

ACKNOWLEDGMENTS

Not Available. Open Access funding enabled and organized by Projekt DEAL.

FUNDING INFORMATION

This work was funded in part by funds obtained from the German Research Foundation (DFG) (clinical research unit “Clinical relevance of tumor-microenvironment interactions in pancreatic cancer” - DFG-KFO325) to DKB, TMG, SB, and MB.

CONFLICT OF INTEREST

The authors declare no competing financial interests.

DATA AVAILABILITY

Data are available on request from the authors.

ORCID

Marina Tatura  <https://orcid.org/0000-0003-3150-8600>

REFERENCES

- Siegel RL, Miller KD, Jemal A. Cancer statistics, 2020. *CA Cancer J Clin*. 2020;70(1):7-30. doi:10.3322/caac.21590
- Singhi AD, Koay EJ, Chari ST, Maitra A. Early detection of pancreatic cancer: opportunities and challenges. *Gastroenterology*. 2019;156(7):2024-2040. doi:10.1053/j.gastro.2019.01.259
- Strobel O, Neoptolemos J, Jager D, Buchler MW. Optimizing the outcomes of pancreatic cancer surgery. *Nat Rev Clin Oncol*. 2019;16(1):11-26. doi:10.1038/s41571-018-0112-1
- Gong T, Liu L, Jiang W, Zhou R. DAMP-sensing receptors in sterile inflammation and inflammatory diseases. *Nat Rev Immunol*. 2020;20(2):95-112. doi:10.1038/s41577-019-0215-7
- Jung S, von Thülen T, Yang I, et al. A ribosomal RNA fragment with 2',3'-cyclic phosphate and GTP-binding activity acts as RIG-I ligand. *Nucleic Acids Res*. 2020;48(18):10397-10412. doi:10.1093/nar/gkaa739
- Heil F, Hemmi H, Hochrein H, et al. Species-specific recognition of single-stranded RNA via toll-like receptor 7 and 8. *Science*. 2004;303(5663):1526-1529. doi:10.1126/science.1093620
- Diebold SS, Kaisho T, Hemmi H, Akira S, Reis e Sousa C. Innate antiviral responses by means of TLR7-mediated recognition of single-stranded RNA. *Science*. 2004;303(5663):1529-1531. doi:10.1126/science.1093616
- Lund JM, Alexopoulou L, Sato A, et al. Recognition of single-stranded RNA viruses by toll-like receptor 7. *Proc Natl Acad Sci U S A*. 2004;101(15):5598-5603. doi:10.1073/pnas.0400937101
- Ostendorf T, Zillinger T, Andryka K, et al. Immune sensing of synthetic, bacterial, and protozoan RNA by toll-like receptor 8 requires coordinated processing by RNase T2 and RNase 2. *Immunity*. 2020;52(4):591-605 e6. doi:10.1016/j.immuni.2020.03.009
- Greulich W, Wagner M, Gaidt MM, et al. TLR8 is a sensor of RNase T2 degradation products. *Cell*. 2019;179(6):1264.e13-1275.e13. doi:10.1016/j.cell.2019.11.001
- Hemmi H, Takeuchi O, Kawai T, et al. A toll-like receptor recognizes bacterial DNA. *Nature*. 2000;408(6813):740-745. doi:10.1038/35047123
- Bauer S, Kirschning CJ, Hacker H, et al. Human TLR9 confers responsiveness to bacterial DNA via species-specific CpG motif recognition. *Proc Natl Acad Sci U S A*. 2001;98(16):9237-9242. doi:10.1073/pnas.161293498
- Jurk M, Heil F, Vollmer J, et al. Human TLR7 or TLR8 independently confer responsiveness to the antiviral compound R-848. *Nat Immunol*. 2002;3(6):499. doi:10.1038/ni0602-499
- Mantovani A, Sica A. Macrophages, innate immunity and cancer: balance, tolerance, and diversity. *Curr Opin Immunol*. 2010;22(2):231-237. doi:10.1016/j.coi.2010.01.009
- Beatty GL, Winograd R, Evans RA, et al. Exclusion of T cells from pancreatic carcinomas in mice is regulated by Ly6C(low) F4/80(+) extratumoral macrophages. *Gastroenterology*. 2015;149(1):201-210. doi:10.1053/j.gastro.2015.04.010
- Kalbasi A, Komar C, Tooker GM, et al. Tumor-derived CCL2 mediates resistance to radiotherapy in pancreatic ductal adenocarcinoma. *Clin Cancer Res*. 2017;23(1):137-148. doi:10.1158/1078-0432.CCR-16-0870
- Griesmann H, Drexel C, Milosevic N, et al. Pharmacological macrophage inhibition decreases metastasis formation in a genetic model of pancreatic cancer. *Gut*. 2017;66(7):1278-1285. doi:10.1136/gutjnl-2015-310049
- Duewell P, Steger A, Lohr H, et al. RIG-I-like helicases induce immunogenic cell death of pancreatic cancer cells and sensitize tumors toward killing by CD8(+) T cells. *Cell Death Differ*. 2014;21(12):1825-1837. doi:10.1038/cdd.2014.96
- Behm B, Di Fazio P, Michl P, et al. Additive antitumor response to the rabbit VX2 hepatoma by combined radio frequency ablation and toll like receptor 9 stimulation. *Gut*. 2016;65(1):134-143. doi:10.1136/gutjnl-2014-308286
- Zambirinis CP, Levie E, Nguy S, et al. TLR9 ligation in pancreatic stellate cells promotes tumorigenesis. *J Exp Med*. 2015;212(12):2077-2094. doi:10.1084/jem.20142162
- Ochi A, Graffeo CS, Zambirinis CP, et al. Toll-like receptor 7 regulates pancreatic carcinogenesis in mice and humans. *J Clin Invest*. 2012;122(11):4118-4129. doi:10.1172/JCI63606
- Michaelis KA, Norgard MA, Zhu X, et al. The TLR7/8 agonist R848 remodels tumor and host responses to promote survival in pancreatic cancer. *Nat Commun*. 2019;10(1):4682. doi:10.1038/s41467-019-12657-w
- Iwamura T, Caffrey TC, Kitamura N, Yamanari H, Setoguchi T, Hollingsworth MA. P-selectin expression in a metastatic pancreatic tumor cell line (SUIT-2). *Cancer Research*. 1997;57(6):1206-1212.
- Ottaviani S, Stebbing J, Frampton AE, et al. TGF-beta induces miR-100 and miR-125b but blocks let-7a through LIN28B controlling PDAC progression. *Nature Communications*. 2018;9(1):1845. doi:10.1038/s41467-018-03962-x
- Kaistha BP, Honstein T, Muller V, et al. Key role of dual specificity kinase TTK in proliferation and survival of pancreatic cancer cells. *Br J Cancer*. 2014;111(9):1780-1787. doi:10.1038/bjc.2014.460
- Kaistha BP, Lorenz H, Schmidt H, et al. PLAC8 localizes to the inner plasma membrane of pancreatic cancer cells and regulates cell growth and disease progression through critical cell-cycle regulatory pathways. *Cancer Res*. 2016;76(1):96-107. doi:10.1158/0008-5472.CAN-15-0216
- Hemmi H, Kaisho T, Takeuchi O, et al. Small anti-viral compounds activate immune cells via the TLR7 MyD88-dependent signaling pathway. *Nat Immunol*. 2002;3(2):196-200. doi:10.1038/ni758

28. Hingorani SR, Wang L, Multani AS, et al. Trp53R172H and KrasG12D cooperate to promote chromosomal instability and widely metastatic pancreatic ductal adenocarcinoma in mice. *Cancer Cell*. 2005;7(5):469-483. doi:10.1016/j.ccr.2005.04.023
29. Anders S, Pyl PT, Huber W. HTSeq-a python framework to work with high-throughput sequencing data. *Bioinformatics*. 2015;31(2):166-169. doi:10.1093/bioinformatics/btu638
30. Mi H, Ebert D, Muruganujan A, et al. PANTHER version 16: a revised family classification, tree-based classification tool, enhancer regions and extensive API. *Nucleic Acids Res*. 2021;49(D1):D394-D403. doi:10.1093/nar/gkaa1106
31. Yu P, Lubben W, Slomka H, et al. Nucleic acid-sensing toll-like receptors are essential for the control of endogenous retrovirus viremia and ERV-induced tumors. *Immunity*. 2012;37(5):867-879. doi:10.1016/j.immuni.2012.07.018
32. Bath-Hextall F, Ozolins M, Armstrong SJ, et al. Surgical excision versus imiquimod 5% cream for nodular and superficial basal-cell carcinoma (SINS): a multicentre, non-inferiority, randomised controlled trial. *Lancet Oncol*. 2014;15(1):96-105. doi:10.1016/S1470-2045(13)70530-8
33. Camargo JA, Passos GR, Ferrari KL, Billis A, Saad MJA, Reis LO. Intravesical immunomodulatory Imiquimod enhances bacillus Calmette-Guerin downregulation of nonmuscle-invasive bladder cancer. *Clin Genitourin Cancer*. 2018;16(3):e587-e593. doi:10.1016/j.clgc.2017.10.019
34. Gao D, Li W, Wang W, et al. Synergy of purine-scaffold TLR7 agonist with doxorubicin on systemic inhibition of lymphoma in mouse model. *J Cancer*. 2017;8(16):3183-3189. doi:10.7150/jca.20015
35. Schmid D, Park CG, Hartl CA, et al. T cell-targeting nanoparticles focus delivery of immunotherapy to improve antitumor immunity. *Nat Commun*. 2017;8(1):1747. doi:10.1038/s41467-017-01830-8
36. Helminen O, Huhta H, Kauppila JH, Lehenkari PP, Saarnio J, Karttunen TJ. Localization of nucleic acid-sensing toll-like receptors in human and mouse pancreas. *APMIS*. 2017;125(2):85-92. doi:10.1111/apm.12632
37. Grimmig T, Matthes N, Hoeland K, et al. TLR7 and TLR8 expression increases tumor cell proliferation and promotes chemoresistance in human pancreatic cancer. *Int J Oncol*. 2015;47(3):857-866. doi:10.3892/ijo.2015.3069

SUPPORTING INFORMATION

Additional supporting information can be found online in the Supporting Information section at the end of this article.

How to cite this article: Stark M, Nicolai M, Tatura M, et al. Dissecting the role of toll-like receptor 7 in pancreatic cancer. *Cancer Med*. 2023;12:8542-8556. doi:10.1002/cam4.5606